

## **SUSTAINED LOADING STRENGTH OF CONCRETE MODELLED BY CREEP-CRACKING INTERACTION**

### **DAUERSTANDFESTIGKEIT VON BETON ALS KRIECHSCHÄDIGUNGSINTERAKTION ABGEBILDET**

### **LA RESISTANCE DU BETON AUX CHARGES SOUTENUES DECRITE PAR L'INTERACTION FLUAGE-FISSURATION**

Joško Ožbolt and Hans-Wolf Reinhardt

#### **SUMMARY**

In the present paper the microplane model for concrete is coupled in series with a linear creep model. The results show that the model is able to account for the creep-cracking interaction. Compared with the instantaneous compressive strength, the strength under sustained load is reduced by about 30%. The tensile resistance under sustained load seems to be highly sensitive to the imperfection of the test specimen. It is shown that the inhomogeneity of the stress-strain field and the realistic modelling of concrete play an important role in the analysis of creep-cracking interaction.

#### **ZUSAMMENFASSUNG**

Im vorliegenden Aufsatz wurde das "Microplane model" für Beton mit einem linearen Kriechmodell in Serie geschaltet. Die Ergebnisse zeigen, dass das Modell die Interaktion von Schädigung und Kriechen gut wiedergibt. Verglichen mit der Kurzzeitdruckfestigkeit ist Dauerstandfestigkeit 30% niedriger. Die Zugfestigkeit unter Dauerlast scheint sehr empfindlich auf Imperfektionen des Prüfkörpers zu reagieren. Es wird gezeigt, dass Spannungsinhomogenitäten in der Beanspruchung und die wirklichkeitsnahe Modellierung von Beton bei der Berechnung von Kriechschädigung eine wichtige Rolle spielen.

#### **RESUME**

Dans l'article présent, le modèle "microplane" pour le béton est monté en série avec un modèle linéaire du fluage. Les résultats prouvent que le modèle résultant peut expliquer l'interaction entre la dégradation et le fluage. Par rapport à la résistance à la compression à court terme, la résistance à la compression

soutenue est inférieure d'environ 30%. La résistance à la traction soutenue semble être extrêmement sensible aux imperfections de l'échantillon. Il est démontré que les inhomogénéités de contrainte et la modélisation réaliste du béton jouent un rôle important dans l'analyse de l'interaction fluage-fissuration.

KEYWORDS: Sustained loading, concrete, compression, tension, creep, damage

## INTRODUCTION

One important aspect of durability of concrete and reinforced concrete structures is the interaction between cracking and creep of concrete. It is well known that the ultimate resistance of a concrete member under sustained load, compared with the resistance of the same member loaded by instantaneous static load, could be considerably smaller. One of the reasons may be creep-cracking interaction which, at constant load, leads to an increase of damage zones and reduction of the ultimate capacity. This effect is even stronger if the structure was previously loaded by cyclic loading.

During the last two decades significant progress in modelling of fracture and damage of concrete-like materials has been done. However, how to describe creep rupture of concrete theoretically has not been dealt with until recently. In the present paper it is investigated whether by coupling of realistic three-dimensional model for concrete (microplane model) with a linear creep model is possible to predict creep-cracking interaction correctly.

## CREEP FRACTURE OF CONCRETE

It is well known that the concrete deformation and strength under sustained load are influenced by the material and geometrical defects, i.e. larger initial flaws lead to lower strength at sustained load. Following this argument, the main assumption in the present approach is that the non-linear creep of concrete is a consequence of the redistribution of stresses due to creep and with this related increase of damage. The redistribution takes place between stronger (less damaged) and weaker (more damaged) zones of the material. Their existence depends on the inhomogeneity of concrete, on the structural geometry as well as on the loading. When such zones do not exist (homogeneity of the stress-strain field), no redistribution of stresses is possible and consequently there is no non-linear creep. When the constitutive law accounts for the existence of these zones

then the coupling of such a constitutive relationship with the linear creep law should be able to predict the effect of non-linear creep.

To confirm the above discussed assumption, in the present paper the microplane model for concrete is coupled in series with the Maxwell chain model (see Figure 1). In an incremental iterative procedure, at time  $t_r$  the stress increment  $\Delta\sigma_r$  is calculated from the known total strain increment  $\Delta\varepsilon_r$  based on the microplane model as:

$$\Delta\sigma_r = \mathbf{D}_r (\Delta\varepsilon_r - \Delta\varepsilon_r'') \quad (1)$$

in which  $\Delta\varepsilon_r''$  is the creep strain increment, calculated from the linear creep law (Maxwell chain model), and  $\mathbf{D}_r$  is the material stiffness tensor obtained from the microplane model. It is assumed that the microplane model parameters are time independent.

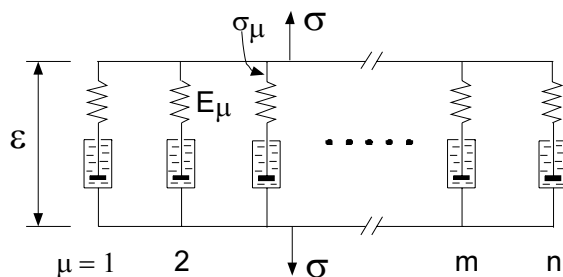


Figure 1. Maxwell chain model.

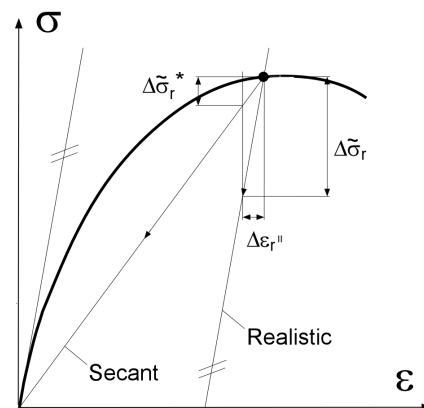


Figure 2. Realistic modelling of concrete for loading-unloading-reloading stress-strain history.

One important point in the modelling of the non-linear creep is that the constitutive law (in our case microplane model) must be able to realistically model concrete response for cyclic loading history, i.e. realistic loading-unloading-reloading rules have to be employed. By the use of a simple secant loading-unloading rule (see Figure 2), what is common in the non-linear analysis of concrete and reinforced concrete structures, it is not possible to account for the effect of non-linear creep. Namely, for relatively high stress levels the

unbalanced stresses of the  $i$ -th iteration step are too low in comparison to the stresses obtained from a realistic constitutive stress-strain law (compare secant and realistic unloading rule in Figure 2). In such a case it is not possible to realistically reproduce the redistribution of stresses in the material. Consequently, the effect of non-linear creep can not be accounted for.

### Microplane model

The microplane model is a three-dimensional macroscopic constitutive law. In the model the material is characterised by a uniaxial relations between the stress and strain components on planes of various orientations. At each integration point these planes may be imagined to represent the damage planes or weak planes of the microstructure. The tensorial invariance restrictions need not be directly enforced. Superimposing the responses from all microplanes in a suitable manner automatically satisfies them. The basic concept behind the microplane model was advanced in 1938 by G.I. Taylor [Taylor 1938]. Later the model was extended by Bažant and co-workers for modelling quasi-brittle materials which exhibit softening [Bažant and Gambarova 1984], [Bažant and Prat 1988]. In the present paper an advanced version of the microplane model for concrete proposed by [Ožbolt et al. 2001] is used. The model is based on the so called "relaxed kinematic constraint" concept. For more detail see [Ožbolt et al. 2001].

### Rate-type creep law of ageing concrete – Maxwell chain

Creep of concrete is modelled by the Maxwell chain model (see Figure 1). It is assumed that the Poisson's ratio due to creep is the same as the elastic one. At time  $t_r$  the total strain increment is decomposed into elastic ( $\Delta\epsilon_r^{el}$ ), cracking ( $\Delta\epsilon_r^{cr}$ ) and creep ( $\Delta\epsilon_r''$ ) strain increments as:

$$\Delta\epsilon_r = \Delta\epsilon_r^{el} + \Delta\epsilon_r^{cr} + \Delta\epsilon_r'' \quad (2)$$

The elastic and damage strains are calculated from the microplane model whereas the creep strains are obtained from the Maxwell chain model. Creep deformations are calculated by the use of the algorithm for step-by-step integration proposed by [Bažant and Wu 1974]. For time step  $\Delta t_r$  the creep strain increments  $\Delta\epsilon_r''$  are calculated as:

$$\Delta \epsilon_r'' = \frac{1}{E_r''} \left( \sum_{\mu=1}^m \left\{ 1 - e^{-\Delta t_r / \tau_\mu} \right\} \sigma_{\mu_{r-1}} \right) \quad (3)$$

with,

$$E_r'' = \sum_{\mu=1}^m \lambda_{\mu_r} E_{\mu_{r-1/2}} + E_{\infty_{r-1/2}} \quad \text{where} \quad E_{\mu_{r-1/2}} = \frac{1}{2} (E_{\mu_{r-1}} + E_{\mu_r})$$

$$\sigma_{\mu_r} = \sigma_{\mu_{r-1}} e^{-\Delta t_r / \tau_\mu} + \lambda_{\mu_{r-1}} E_{\mu_{r-1/2}} (\Delta \epsilon_r - \Delta \epsilon_r^{cr}) \quad (4)$$

$$\lambda_{\mu_r} = (1 - e^{-\Delta t_r / \tau_\mu}) \tau_\mu / \Delta t_r$$

in which  $\mu$  denotes  $\mu$ -th unit of the Maxwell chain model,  $\tau_\mu = \eta_\mu / E_\mu$  is the relaxation time of the unit,  $\eta_\mu$  and  $E_\mu$  are viscosity and modulus of the  $\mu$ -th unit, respectively,  $\sigma_\mu$  is the so called hidden stresses of the  $\mu$ -th spring unit and  $E_r''$  is pseudo-instantaneous Young's modulus. In the present study the model with eight units is employed.

The main advantage of the rate type formulation over the integral formulation is that the creep deformations are calculated only from the stresses of the previous load step whereas in the integral formulation the entire load history needs to be stored.

## NUMERICAL ANALYSIS OF CREEP-FRACTURE INTERACTION

To investigate whether the coupling of the microplane model for concrete in series with a Maxwell chain model can account for the effect of non-linear creep, three-dimensional finite element analysis of concrete compressive and tensile specimen was carried out. For both specimens the load was applied at an age of 28 days. The linear creep deformation at  $t = \infty$  was taken three times larger than the instantaneous deformation (creep factor  $\varphi = 3$ ). The smeared fracture finite element analysis is carried out by the use of the eight-node solid finite elements with eight integration points. To account for the objectivity of the analysis with respect to the size of the finite elements, the crack band approach was used [Bažant and Oh 1983].

## Uniaxial compression

Creep of concrete under compressive load is analysed for the specimen geometry shown in Figure 3. The basic material properties were as follows: Young's modulus  $E = 28000$  MPa, Poisson's ratio  $\nu = 0.18$ , uniaxial tensile strength  $f_t = 2.0$  MPa, uniaxial compressive strength  $f_c = 28$  MPa, fracture energy  $G_F = 0.10$  N/mm and concrete compressive fracture energy  $G_C = 100G_F$ . The typical uniaxial tensile-compressive stress-strain curve obtained from one three-dimensional finite element, assuming a crack band width of  $h = 20$  mm is shown in Figure 4.

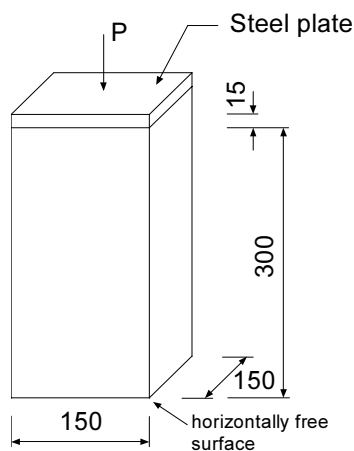


Figure 3. Geometry and boundary conditions of compressive specimen (all in [mm]).

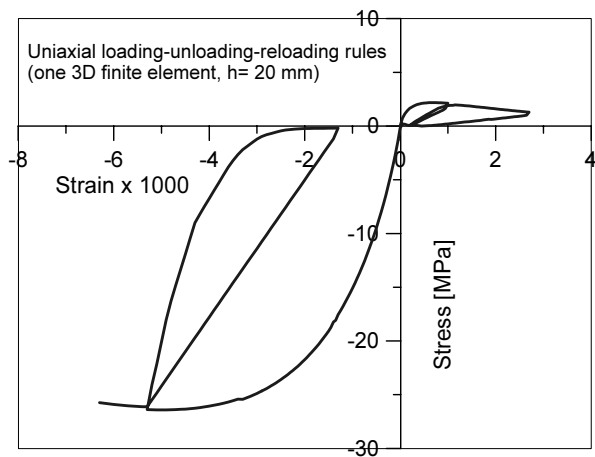


Figure 4. Constitutive law for concrete – uniaxial tensile-compressive relationship obtained from single solid finite element.

The load was applied over a stiff loading platen. It is used because in this way the inhomogeneity of the stress-strain field was generated and it was not necessary to introduce a weak zone or to randomly generate the material properties. First, the average strength of the specimen under instantaneous load was calculated as  $f_c^* = P_U/A$ , where  $P_U$  = ultimate load and  $A$  = cross section area. The load was performed by displacement control. The concrete strength was obtained as  $f_c^* = 24.40$  MPa (note that this strength contains is also a structural effects and is not the same as  $f_c$ ). Subsequently, the time analysis of the specimen loaded by constant compressive load of different levels (load control) was carried out. The sustained load was varied from  $P = 0.6P_U$  to  $P = P_U$ . The maximal duration of the loading was 10000 days. When during this period of time the specimen did not fail it was assumed that the compressive strength under sustained load  $f_{c,s}^*$  was higher.

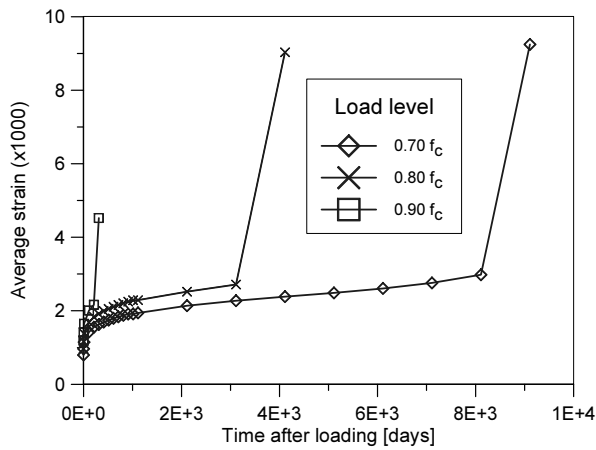


Figure 5. Calculate strain-time relationship for different load levels.

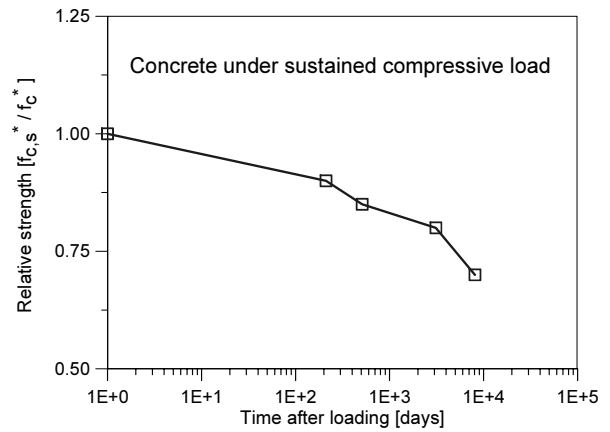


Figure 6. The relation between the relative compressive strength and time at failure.

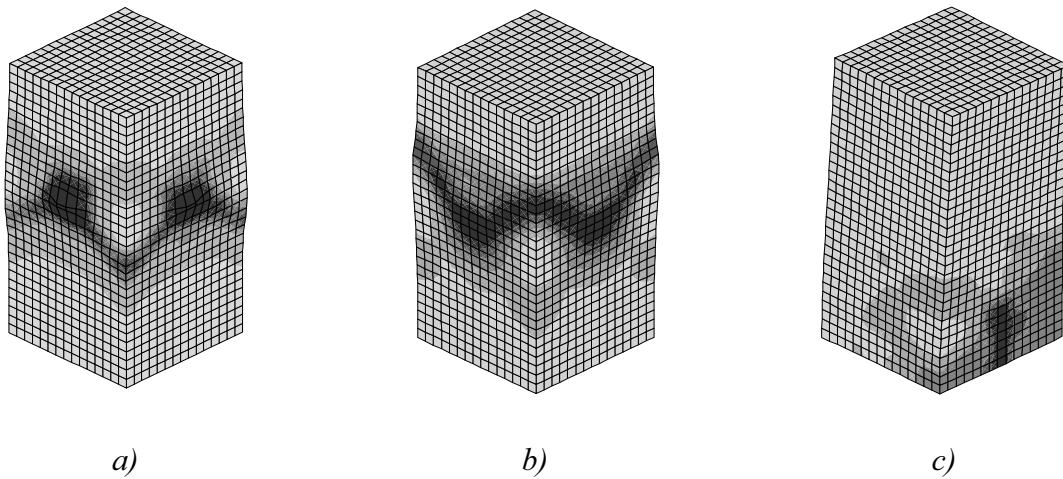


Figure 7. Calculated failure modes (dark zone = maximal principal strains) for: a) instantaneous load, b)  $P = 0.9P_U$  and c)  $P = 0.7P_U$ .

The strength under sustained load is 30% smaller than the compressive instantaneous strength ( $f_{c,s}^* = 0.7f_c^*$ ). The three typical average deformation versus time curves ( $P = 0.7P_U$ ,  $0.8P_U$  and  $0.9P_U$ ) are shown in Figure 5. The curves show that with increase of the load level ( $0.7P_U$  to  $0.9P_U$ ) the creep deformations increase and the time to failure decreases. The calculated relation between the relative compressive strength and duration of load is shown in Figure 6. The typical failure mode due to the instantaneous load is shown in Figure 7a. For comparison, Figures 7b and 7c show the failure mode of the specimen loaded by  $P = 0.9P_U$  (failure after 211 days) and  $0.7P_U$  (failure after 8111 days), respectively.

The above numerical results are similar to the experimental observations, except that it is believed that the compressive strength under sustained load is approximately  $0.8P_U$  and not  $0.7P_U$  as obtained in the present analysis. The reason may be due to the fact that so far no experiment has been performed over a time period of 25 years (specimen loaded with  $0.7P_U$  failed after approximately 25 years) or this may be caused by the fact that in the analysis the ageing effect, i.e. increase of the strength with time was not accounted for. It is interesting to observe that the failure mode of the specimen loaded with  $P = 0.9P_U$  is the same as for the specimen under instantaneous load. However, the specimen loaded by  $P = 0.7P_U$  fails in a different way (compare Figures. 7b and 7c).

### Uniaxial tension

To investigate the creep-fracture interaction for tensile load, the three-dimensional finite element analysis of the specimen shown in Figure 8 was carried out. Figure 9 shows the finite element discretization. The material properties were taken as: Young's modulus  $E = 30000$  MPa, Poisson's ratio  $\nu = 0.18$ , uniaxial tensile strength  $f_t = 2.5$  MPa, uniaxial compressive strength  $f_c = 30$  MPa and fracture energy  $G_F = 0.10$  N/mm. The geometry was chosen such that the specimen fails at the mid-cross section (the weakest section) and that from the beginning of loading no localisation of damage exist (no defect). It was first loaded by displacement control of the right end up to the failure. The calculated tensile strength was  $f_t^* = P_U/A = 2.5$  MPa ( $A$  = critical cross-section area).

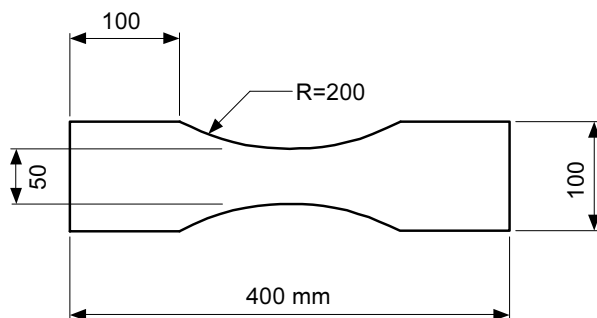


Figure 8. Geometry of the tensile specimen (all in [mm]).

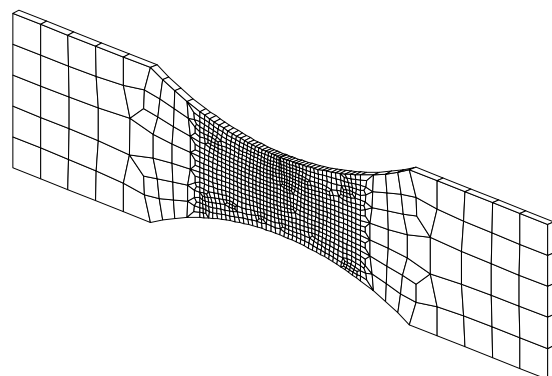


Figure 9. The finite element discretization of the of tensile specimen.



Subsequently, similar as in the case of the compression, the specimen was loaded by sustained load at different load levels. The analysis showed that the tensile strength under sustained load is equal to the instantaneous tensile strength, i.e. no creep-fracture interaction was observed. The reason is probably due to the stress-strain field which was up to the onset of cracking practically homogeneous.

To investigate the influence of the material inhomogeneity, the analysis is repeated but the tensile strength and fracture energy were randomly generated. They were scaled between 80% and 100%. The result was however the same, i.e. as a consequence of creep deformation the damage was distributed over the entire depth of the specimen and over certain width of the critical cross-section, with no clear localisation of damage (see Figure 10). Finally, a notch was introduced at the mid-cross-section of the specimen. The notch size was such that the specimen net cross-section area was reduced by 4%. The results show a strong reduction of the average tensile strength of the specimen under sustained load. For the reduction of the cross-section by 4% the strain under sustained load is obtained as  $f_{t,s}^* = 0.80f_t^*$ . The calculated relations between the relative strength and duration of loading are plotted in Figure 11. Figure 12 shows the crack pattern obtained for sustained load of  $P = 0.8P_U$ .

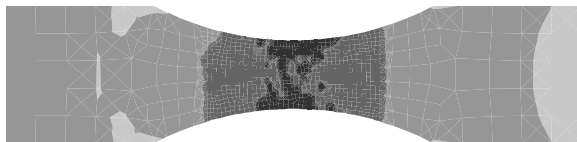


Figure 10. Distribution of damage zones for random concrete properties (dark zones = maximum principal strains),  $P = 0.8P_U$ , time = 10000 days.

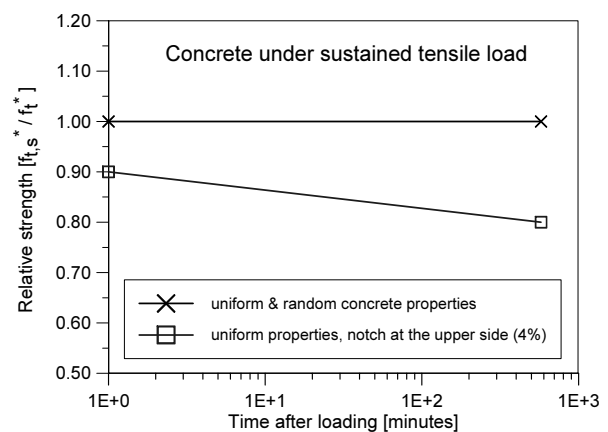


Figure 11. The relation between the relative tensile strength and time at failure.

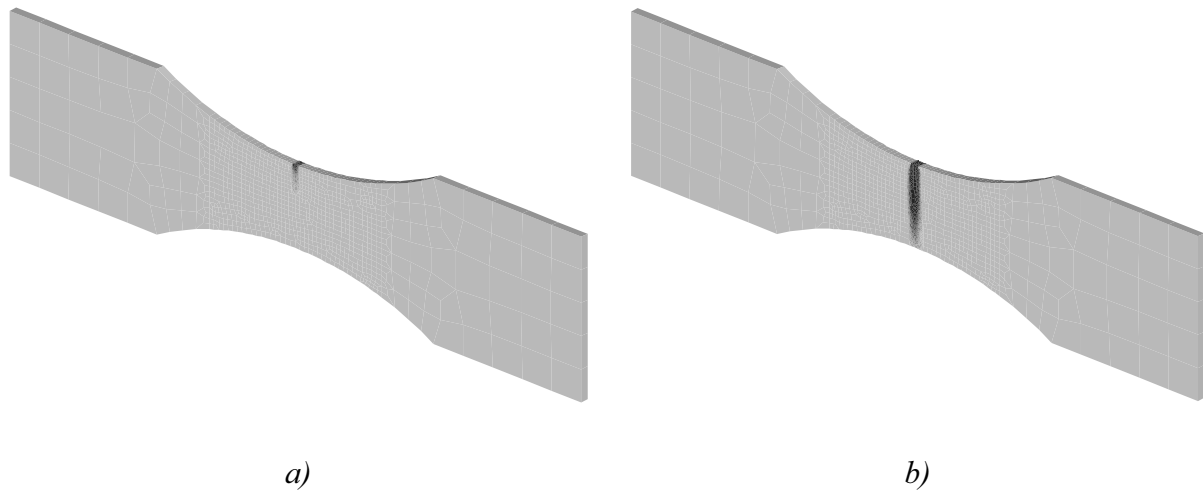


Figure 12. Crack pattern (dark zone = maximum principal strains) for the specimen with  $P = 0.8P_U$  after: a) duration of load = 2.4 hours and b) duration of load = 9.6 hours.

The analysis of the tensile specimen clearly shows the high sensitivity of the tensile specimen on the non-symmetric defect. A strong interaction between damage and creep is observed. It is mainly due to the bending of the specimen which leads to significant reduction of the overall tensile resistance. This indicates that, in experiments, the test set-up might have a strong influence on the measured tensile strength under sustained load. For instance, when the cylindrical tensile specimen is loaded over a glued steel platen it can happen that the unsymmetrical damage localise at the concrete-platen contact what then may lead to the significant scatter of the test results and possibly to their misinterpretation. To prove this further experimental and numerical investigations are needed.

## CONCLUSIONS

In the present paper the microplane model for concrete is coupled in series with the Maxwell chain model in order to investigate whether the resulting model is able to account for the effect of non-linear creep (creep-cracking interaction). The three-dimensional finite element analysis of concrete compressive and tensile specimen was carried out. It is demonstrated that that the present model is able to predict the effects of non-linear creep, i.e. increase of creep deformations at higher stress levels and decrease of the concrete strength for sustained load. The compressive strength of concrete under sustained load is found to be 30% smaller than the strength under instantaneous load. The reason is due to the localisation of damage, as a consequence of

inhomogeneity of the stress-strain field, and resulting redistribution of the stresses due to creep. For the uniaxial tension specimen no significant creep-fracture interaction is obtained as long as the stress-strain field was homogeneous. The same was observed when the random generation of the fracture properties of concrete was introduced. On the contrary, if a small defect in form of a notch was applied a significant creep-fracture interaction is observed. This indicates that the influence of the boundary conditions on the experimental results can be important since small geometrical or material defects can significantly influence the results and possibly lead to the wrong conclusions. The study shows that the correct modelling of creep-fracture interaction is possible only then when the material model for concrete accounts for loading-unloading-reloading stress-strain load history.

## REFERENCES

- [Bažant and Gambarova 1984] Z.P. Bažant and P. Gambarova, Crack shear in concrete: Crack band microplane model, *Journal of Engineering. Mechanics*, ASCE, 110, 2015-2035, (1984).
- [Bažant and Oh 1983] Z.P. Bažant and B.-H. Oh, Crack band theory for fracture of concrete, *Materials and Structures* 16(93), 155-177, (1983).
- [Bažant and Prat 1988] Z.P. Bažant and P.C. Prat, Microplane model for brittle-plastic material - parts I and II, *Journal of Engineering. Mechanics*, ASCE, 114, 1672-1702, (1988).
- [Bažant and Wu 1974] Z.P. Bažant and S.T. Wu, Rate-type creep law of aging concrete based on Maxwell chain, *Materials and Structures* 7(37), 45-59, (1974).
- [Ožbolt et al. 2001] J. Ožbolt, Y.-J Li and I. Kožar, Microplane model for concrete with relaxed kinematic constraint, *International Journal of Solids and Structures*, 38, 2683-2711, (2001).
- [Taylor 1938] G.I. Taylor, Plastic strain in metals, *Journal of the Institute of Metals*, London, (62), 307-324, (1938).

